MIXED FINITE ELEMENT DISCRETIZATION OF CONTINUITY EQUATIONS ARISING IN SEMICONDUCTOR DEVICE SIMULATION

R. HIPTMAIR AND R.H.W. HOPPE *

Summary. In the wake of decoupling and linearization semiconductor device simulation based on van Roosbroecks's equations requires the solution of convection–diffusion equations. It is well known that due to the occurrence of local regions of strong convection standard discretizations do not behave properly. As an alternative among others, mixed methods have been suggested having their roots in the dual variational formulation of the convection–diffusion problem. Their efficient implementation has to make use of Lagrangian multipliers. In a novel approach we already introduce the multiplier prior to discretizing, through a process called hybridization. In the sequel we use the resulting variational problem to develop a new discretization scheme. Next, we outline how to implement a standard mixed scheme and investigate some of its aspects. Finally, the behaviour of the mixed method is illustrated by a series of numerical experiments.

Key words. convection–diffusion problem, flux oriented schemes, hybridization, Lagrangian multipliers, mixed finite elements, Raviart–Thomas elements

MSC subject classifications. Primary 65N30; secondary 35J20

1. Introduction. We consider the linearized current continuity equation in 2–D semiconductor device simulation stated as a drift–diffusion equation for the carrier concentration n

$$\begin{aligned} \operatorname{div}(\nabla n - n\nabla\Psi) - Rn &= f && \text{in } \Omega \\ n &= g && \text{on } \Gamma_D \subset \partial\Omega \\ \frac{\partial n}{\partial \nu} - n\frac{\partial \Psi}{\partial \nu} &= 0 && \text{on } \Gamma_N \subset \partial\Omega \end{aligned} \tag{1}$$

Here $\Omega \subset \mathbf{R}^2$ stands for the cross section of the device, Ψ is the electric potential, R refers to the differential net recombination rate and f denotes a source term. Further, we assume inhomogeneous Dirichlet boundary conditions at the Ohmic contacts $\Gamma_D \subset \Gamma := \partial\Omega$ and homogeneous Neumann boundary conditions at the insulation part Γ_N of the boundary ($\Gamma_N \cup \Gamma_D = \Gamma, \Gamma_N \cap \Gamma_D = \emptyset$). The familiar standard variational (primal) formulation of (1) is:

$$\text{Find } n \in n_0 + H^1_{\Gamma_D}(\Omega) \text{ such that } \quad a_{std}(n,v) = f_{std}(v), \quad v \in H^1_{\Gamma_D}(\Omega) \tag{2}$$

* Mathematisches Institut, Technische Universität München, Arcisstraße 21, D-8000 München 2,e–mail: rohop@mathematik.tu-muenchen.de, hiptmair@mathematik.tu-muenchen.de. The first author was supported by FORTWIHR, Bavarian Consortium for High Performance Scientific Computing

where $H^1_{\Gamma_D}(\Omega)$ contains the functions of $H^1(\Omega)$ with zero trace on Γ_D and $n_0 \in H^1(\Omega)$, $n_0|_{\Gamma_D} = g$ (in the sense of a trace). Additionally we used the bilinear form

$$a_{std} : \begin{cases} H^1(\Omega) \times H^1(\Omega) & \mapsto \mathbf{R} \\ (n, v) & \mapsto \int_\Omega e^\Psi \left\langle \nabla(e^{-\Psi} n), \nabla v \right\rangle d\mathbf{x} + \int_\Omega Rnv \, d\mathbf{x} \end{cases} \tag{3}$$

and right–hand side

$$f_{std} : H^1(\Omega) \mapsto \mathbf{R} \quad ; \quad v \mapsto -\int_\Omega fv \, d\mathbf{x} \tag{4}$$

In view of the identity $e^\Psi \nabla(e^{-\Psi} n) = \nabla n - n\nabla\Psi$ we may introduce the Slotboom variable $u := e^{-\Psi} n$ and get the problem:

$$\begin{aligned} \operatorname{div}(e^\Psi \nabla u) - e^\Psi R u &= f && \text{in } \Omega \\ u &= e^{-\Psi} g && \text{on } \Gamma_D \subset \partial\Omega \\ \tfrac{\partial u}{\partial \boldsymbol{\nu}} &= 0 && \text{on } \Gamma_N \subset \partial\Omega \end{aligned} \tag{5}$$

In this paper we are going to switch frequently between both unknowns. To guide the reader they are invariably denoted by u and n.

By virtue of its symmetric structure (5) can be formulated as an unconstrained minimization problem for the total energy over the space $H^1(\Gamma_D, e^{-\Psi} g) := \{v \in H^1(\Omega); v_{|\Gamma_D} = e^{-\Psi} g\}$:

Find u in $H^1(\Gamma_D, e^{-\Psi} g)$ such that

$$J(u) := \inf_{v \in H^1(\Gamma_D, e^{-\Psi} g)} J(v) \tag{6}$$

where

$$J(v) := \frac{1}{2} \int_\Omega e^\Psi \left(|\nabla v|^2 + R|v|^2 \right) dx + \int_\Omega fv \, d\mathbf{x}.$$

Usually (2) is the starting point for a Galerkin approximation or, more preferably, a Petrov–Galerkin approach which is more suited in case of strong convection because of its upwind features (see for example the streamline diffusion method developed by Hughes et al. in [10]).

On the other hand, for problems where the flux is of primary interest the above formulation is less appropriate, since the current $\mathbf{j} := e^\Psi \nabla u$ must be calculated by differentiation thus resulting in a loss of accuracy. Moreover, for problems with regions of strong convection it may be more advisable to use flux–oriented variational principles that are based on the conservation of the current. Such variational principles can be obtained by duality arguments. In particular, it is well known from convex analysis (see for instance [9])

that the unconstrained minimization of a convex objective functional is equivalent to a saddle point problem in terms of the convex conjugate which constitutes the so–called dual problem (as opposed to the primal problem (2)). For the energy functional J in (6) we can use the obvious identity

$$\frac{1}{2}\int_\Omega |\nabla v|^2\,d\mathbf{x} = \sup_{\mathbf{q}\in(L^2(\Omega))^2}\left\{\int_\Omega \langle \mathbf{q},\nabla v\rangle\,d\mathbf{x} - \frac{1}{2}\int_\Omega |\mathbf{q}|^2\,d\mathbf{x}\right\}$$

together with Green's formula

$$\int_\Omega v\,\mathrm{div}\,\mathbf{q}\,d\mathbf{x} + \int_\Omega \langle \nabla v,\mathbf{q}\rangle\,d\mathbf{x} = \int_\Gamma v\,\langle \mathbf{q},\boldsymbol{\nu}\rangle\,d\Gamma, \quad v\in H^1(\Omega) \quad \mathbf{q}\in\mathbf{H}(\mathrm{div},\Omega)$$

where $\mathbf{H}(\mathrm{div},\Omega) := \{\mathbf{q}\in (L^2(\Omega))^2\,;\mathrm{div}\,\mathbf{q}\in L^2(\Omega)\}$ (We use bold type for vector–valued variables). Setting $\mathbf{H}(\mathrm{div},\Omega,\Gamma_N) := \{\mathbf{q}\in\mathbf{H}(\mathrm{div},\Omega);\langle \mathbf{q},\boldsymbol{\nu}\rangle_{|\Gamma_N}=0\}$, we thus get the dual problem as the following *saddle point problem*:

Find $(\mathbf{j},u)\in\mathbf{H}(\mathrm{div},\Omega,\Gamma_N)\times L^2(\Omega)$ such that

$$L(\mathbf{j},u) = \inf_{\mathbf{v}\in\mathbf{H}(\mathrm{div},\Omega,\Gamma_N)}\ \sup_{w\in L^2(\Omega)} L(\mathbf{v},w) \tag{7}$$

where

$$L(\mathbf{v},w) := \frac{1}{2}\int_\Omega e^{-\Psi}|\mathbf{v}|^2\,d\mathbf{x} + \int_\Omega\left(\mathrm{div}\,\mathbf{v} - \frac{1}{2}e^{\Psi}Rw - f\right)w\,d\mathbf{x} - \int_{\Gamma_D} e^{-\Psi}g\,\langle \mathbf{v},\boldsymbol{\nu}\rangle\,d\Gamma$$

The dual problem (7) is also called the mixed formulation of (5).

A widely used approach to the numerical solution of that mixed formulation is to use mixed finite elements (cf. [7], [8]), a specimen of which are the lowest order Raviart–Thomas elements presented in [11]. Following De Veubeke's smart idea in [13], one subsequently eliminates the continuity constraints for the normal component of the discrete fluxes at the interelement boundaries from the discrete flux space by means of appropriate *Lagrangian multipliers*. Static condensation and rescaling then leads to a Schur complement system which is related to a specific nonconforming finite element method. This hybridization of the mixed discretization has been theoretically analyzed by Brezzi at al. (cf. [6], [1]) and has recently been implemented by Reusken (cf. [12]) within a multigrid framework.

So far De Veubeke's trick has only been employed after discretization had already been completed. To our mind a quite appealing alternative is to apply hybridization directly to the dual formulation which results in some sort of continuous analogue of the Schur complement. As the side–effects of a particular discretization do not have to be taken into account this approach may reward us with additional insights into the genuine properties of the problems. As the continuous problem is subject to spectral analysis, prospects

arise to gain important information about appropriate preconditioning. Note that in classical domain decomposition a related approach, namely hybridization of the primal problem has been investigated by Bjørstad and Widlund in [4].

The remainder of the paper is organized as follows: In section 2 we will give the mixed formulation of (1) and present the details of dual hybridization. A spectral analysis of the dual hybrid operator is then carried out for a simple model problem. The next section is devoted to a special flux–oriented upwind scheme that is related to the discretization technique of Baliga–Patankar (cf. [2]). In section 4 we are reviewing some aspects of the standard mixed discretization and its relationship to inverse average type nonconforming Petrov–Galerkin methods. Finally, in section 5 we are presenting the results of a couple of numerical experiments which center on the performance of the mixed method in special situations.

2. Dual Hybridization. The variational equations arising from the mixed saddle point problem (7) by means of Gâteaux differentiation of the functional L with respect to both variables read:

Find $(\mathbf{j}, u) \in \mathbf{H}(\mathrm{div}, \Omega, \Gamma_N) \times L^2(\Omega)$ such that

$$\begin{array}{rcrcll} \int_\Omega e^{-\Psi}\langle \mathbf{j}, \mathbf{v}\rangle \, d\mathbf{x} & + & \int_\Omega u \,\mathrm{div}\, \mathbf{v} \, d\mathbf{x} & = & \int_{\Gamma_D} e^{-\Psi} g \,\langle \mathbf{v}, \boldsymbol{\nu}\rangle \, d\Gamma, & \mathbf{v} \in \mathbf{H}(\mathrm{div}, \Omega, \Gamma_N) \\ \int_\Omega w \,\mathrm{div}\, \mathbf{j} \, d\mathbf{x} & - & \int_\Omega e^{\Psi} R u w \, d\mathbf{x} & = & \int_\Omega f w \, d\mathbf{x}, & w \in L^2(\Omega) \end{array} \tag{8}$$

Another derivation of (8) immediately replaces $e^{\Psi}\nabla u$ in (5) by the new variable $\mathbf{j}$ (the flux) and thus converts (5) into a first order system of partial differential equations:

$$\left.\begin{array}{r} \mathbf{j} = e^{\Psi}\nabla u \\ \mathrm{div}\,\mathbf{j} - e^{\Psi} R u = f \end{array}\right\} \text{ in } \Omega \qquad \begin{array}{rcll} u & = & e^{-\Psi} g & \text{on } \Gamma_D \\ \langle \mathbf{j}, \boldsymbol{\nu}\rangle & = & 0 & \text{on } \Gamma_N \end{array} .$$

Both equations are now written in variational form and applying Green's formula we arrive at (8). We can take our cue from these considerations to prove that both the mixed problem (8) and its standard counterpart (2) do yield the same solutions apart from scaling.

The main objective of hybridization is to get rid of the global space $\mathbf{H}(\mathrm{div}, \Omega, \Gamma_N)$. It is a common experience — see for instance [11] —, that its discrete analogues are not easily handled. The tool of a Lagrangian multiplier enables us to break up the space into less bulky pieces. The splitting of the space $\mathbf{H}(\mathrm{div}, \Omega, \Gamma_N)$ is based on a decomposition of Ω, a "generalized triangulation" $\mathcal{T}_h := \{T_i\}_{i=1}^N$ ($N \in \mathbb{N}$): The patches T_i are open, nonempty convex subsets, mutually disjoint and the union of their closures entirely covers Ω. Furthermore we demand that they align with the boundary parts. A general triangulation of this kind is feasible as long as Ω has polygonal boundary and all internal boundaries

have to be straight lines. In the sequel this is always taken for granted. For convenience we write $\mathcal{E}$ to refer to the union of edges of the $T_\imath$.

A fundamental result (cf. [6]) now states that a "fragmented" vector field in $\boldsymbol{\mathcal{X}} := \bigotimes_\imath \mathbf{H}(\mathrm{div}, T_\imath)$ belongs to $\mathbf{H}(\mathrm{div}, \Omega, \Gamma_N)$ if and only if its normal components at the internal boundaries of $\mathcal{T}$ are continuous and do vanish on Γ_N. Hence, any Lagrangian multiplier meant to single out members of $\mathbf{H}(\mathrm{div}, \Omega, \Gamma_N)$ has to enforce the continuity of the normal components across the joint edge of two patches. We do not want to dip into details here: A careful analysis reveals that $\mathcal{M} := H^1_{\Gamma_D}(\Omega)$ is a suitable space of multipliers. Of course, for an $m \in \mathcal{M}$ only the traces on $\mathcal{E}$ are relevant. Now, by means of the multiplier space $\mathcal{M}$ an element $\mathbf{v} \in \boldsymbol{\mathcal{X}}$ lives in $\mathbf{H}(\mathrm{div}, \Omega, \Gamma_N)$ if and only if

$$l(\mathbf{v}, m) = 0, \quad m \in \mathcal{M} \tag{9}$$

with $l : \boldsymbol{\mathcal{X}} \times \mathcal{M} \mapsto \mathbb{R}$ denoting the bilinear mapping

$$l(\mathbf{v}, m) := -\sum_{\imath=1}^{N} \int_{\partial T_\imath} \left\langle \mathbf{v}_{|T_\imath}, \boldsymbol{\nu} \right\rangle m \, d\Gamma \, .$$

(7) and (9) are now merged into an augmented saddle point problem: Find $(\mathbf{j}, u, p) \in \boldsymbol{\mathcal{X}} \times \mathcal{W} \times \mathcal{M}$ such that

$$\tilde{L}(\mathbf{j}, u, p) = \sup_{w \in \mathcal{W}} \inf_{\mathbf{v} \in \boldsymbol{\mathcal{X}}} \sup_{m \in \mathcal{M}} \tilde{L}(\mathbf{v}, w, m) \tag{10}$$

where $\tilde{L}(\mathbf{v}, w, m,) := L(\mathbf{v}, w) + l(\mathbf{v}, m)$ and $\mathcal{W}$ served as an abbreviation for $L^2(\Omega)$. For the sake of accuracy we should point out that L (cf. (7)) is assumed to be extended to functions in $\boldsymbol{\mathcal{X}}$ in a canonical fashion. Once more, Gâteaux differentiation of (10) is quickly done and yields the *mixed hybrid problem*

Find $(\mathbf{j}, u, p) \in \boldsymbol{\mathcal{X}} \times \mathcal{W} \times \mathcal{M}$ such that

$$\begin{array}{lllllll} a(\mathbf{j}, \mathbf{v}) & + & b(\mathbf{v}, u) & + & l(\mathbf{v}, p) & = & g(\mathbf{v}) \, , \quad \mathbf{v} \in \boldsymbol{\mathcal{X}} \\ b(\mathbf{j}, w) & - & d(u, w) & & & = & f(w) \, , \quad w \in \mathcal{W} \\ l(\mathbf{j}, m) & & & & & = & 0 \, , \quad m \in \mathcal{M} \end{array} \tag{11}$$

where

$$a(\mathbf{j}, \mathbf{v}) := \int_\Omega e^{-\Psi} \langle \mathbf{j}, \mathbf{v} \rangle \, d\mathbf{x} \, , \; b(\mathbf{v}, u) := \sum_\imath \int_{T_\imath} u \, \mathrm{div}\, \mathbf{v} \, d\mathbf{x} \, , \; d(u, w) := \int_\Omega e^{\Psi} R u w \, d\mathbf{x}$$

and

$$g(\mathbf{v}) := \int_{\Gamma_D} e^{-\Psi} g \, \langle \mathbf{v}, \boldsymbol{\nu} \rangle \, d\Gamma \, , \; f(w) := \int_\Omega f w \, d\mathbf{x} \quad .$$

Standard techniques developed for general saddle point problems (cf. [6]) establish existence and uniqueness of a solution of (11); uniqueness of p is to be understood as a statement about its traces on $\mathcal{E}$.

As an elementary but interesting feature of (11) we wish to mention that the components u and p of the solution have the same trace on $\mathcal{E}$. First of all, this fact teaches us how to write (11) for the original unknown n: Just replace u and p by $e^{\Psi}u$ and $e^{\Psi}p$, respectively. This observation is also numerically significant: As soon as an approximation of p is available, one of u is also known on the edges.

Each bilinear form of (11) can be associated with a Riesz operator denoted by the respective capital letter. Their adjoints are marked by an asterisk. Writing (11) as an equation for operators in function spaces we then obtain the following system:

$$\begin{pmatrix} A & B^* & L^* \\ B & -D & 0 \\ L & 0 & 0 \end{pmatrix} \begin{pmatrix} \mathbf{j} \\ u \\ p \end{pmatrix} = \begin{pmatrix} g \\ f \\ 0 \end{pmatrix} \tag{12}$$

2.1. The Dual–Hybrid Variational Problem. Due to its special structure the system (12) lends itself to static condensation in a wider sense: Through a process similar to block elimination of linear systems we seek to dump all unknowns except for p. Doing so produces the following equation:

$$\begin{pmatrix} L \\ 0 \end{pmatrix} \begin{pmatrix} A & B^* \\ B & -D \end{pmatrix}^{-1} \begin{pmatrix} L \\ 0 \end{pmatrix}^* p = \begin{pmatrix} L \\ 0 \end{pmatrix} \begin{pmatrix} A & B^* \\ B & -D \end{pmatrix}^{-1} \begin{pmatrix} g \\ f \end{pmatrix}$$

which we are going to write as $Sp = q$.

To go beyond playing with symbols we are now scrutinizing the related variational problem: Find $p \in \mathcal{M}$ such that

$$\langle Sp, m \rangle_{\mathcal{M}' \times \mathcal{M}} = q(m), \quad m \in \mathcal{M} \tag{13}$$

by untangling the left hand side: (As usual, dual spaces are marked by a prime ')

- First $\binom{L}{0}^* p \in (\boldsymbol{\mathcal{X}} \times \mathcal{W})'$ for $p \in \mathcal{M}$ is given by

$$\begin{pmatrix} L \\ 0 \end{pmatrix}^* p \begin{pmatrix} \mathbf{v} \\ w \end{pmatrix} = -\sum_{i=1}^{N} \int_{\partial T_i} p \left\langle \mathbf{v}_{|T_i}, \boldsymbol{\nu} \right\rangle d\Gamma = l(\mathbf{v}, p) \,, \qquad \begin{pmatrix} \mathbf{v} \\ w \end{pmatrix} \in \boldsymbol{\mathcal{X}} \times \mathcal{W}$$

- Evaluating $\begin{pmatrix} A & B^* \\ B & -D \end{pmatrix}^{-1} \begin{pmatrix} h_1 \\ h_2 \end{pmatrix} \in \boldsymbol{\mathcal{X}} \times \mathcal{W}$ for $h_1 \in \boldsymbol{\mathcal{X}}', h_2 \in \mathcal{W}'$ is equivalent to the variational problem:

  Find $(\mathbf{j}, u) \in \boldsymbol{\mathcal{X}} \times \mathcal{W}$ such that

$$\begin{array}{rcrcll} a(\mathbf{j}, \mathbf{v}) & + & b(\mathbf{v}, u) & = & h_1(\mathbf{v}), & \mathbf{v} \in \boldsymbol{\mathcal{X}} \\ b(\mathbf{j}, w) & - & d(u, w) & = & h_2(w), & w \in \mathcal{W} \end{array} \tag{14}$$

Now, we are witnessing the crucial benefit of hybridization: The main purpose of introducing a multiplier was *decoupling*: Writing $\mathbf{v} = \sum_i \mathbf{v}_i, \mathbf{v}_i \in \mathbf{H}(\mathrm{div}, T_i, \Gamma_N)$ and $w = \sum_i w_i, w_i \in L^2(T_i)$ (14) spawns a host of variational problems:

Find $(\mathbf{j}_i, u_i) \in \mathbf{H}(\mathrm{div}, T_i, \Gamma_N) \times L^2(T_i)$ such that

$$\begin{array}{rcrcll} a(\mathbf{j}_i, \mathbf{v}_i) & + & b(\mathbf{v}_i, u_i) & = & \tilde{h}_1(\mathbf{v}_i), & \mathbf{v}_i \in \mathbf{H}(\mathrm{div}, T_i, \Gamma_N) \\ b(\mathbf{j}_i, w_i) & - & d(u_i, w_i) & = & \tilde{h}_2(w_i), & w_i \in L^2(T_i) \quad . \end{array} \qquad 1 \le i \le N \quad (15)$$

Since we have disposed of all the continuity ties between the $\mathbf{v}_i$, these problems can be solved independently.

- Finally, $\binom{L}{0}\binom{v}{w}$ with $\binom{v}{w} \in \boldsymbol{\mathcal{X}} \times \mathcal{W}$ is a linear form on $\mathcal{M}$:

$$\begin{pmatrix} L \\ 0 \end{pmatrix} \begin{pmatrix} \mathbf{v} \\ w \end{pmatrix} p = l(\mathbf{v}, p) = -\sum_{i=1}^{N} \int_{\partial T_i} p \, \langle \mathbf{v}, \boldsymbol{\nu} \rangle \, d\Gamma, \quad p \in \mathcal{M} \quad .$$

In sum, the evaluation of $\langle Sp, m \rangle_{\mathcal{M}' \times \mathcal{M}}$ requires basically two steps:

1. As a first step for each $T_i \in \mathcal{T}$ we have to solve

   Find $(\mathbf{j}_i, u_i) \in \mathbf{H}(\mathrm{div}, T_i, \Gamma_N) \times \mathrm{L}^2(T_i)$ such that

$$\begin{array}{rcrcll} a(\mathbf{j}_i, \mathbf{v}_i) & + & b(\mathbf{v}_i, u_i) & = & -l(\mathbf{v}_i, p)\,, & \mathbf{v}_i \in \mathbf{H}(\mathrm{div}, T_i, \Gamma_N) \\ b(\mathbf{j}_i, w_i) & - & d(u_i, w_i) & = & 0\,, & w_i \in \mathrm{L}^2(T_i) \end{array} \qquad 1 \le i \le N (16)$$

   Recalling (7) these problems turn out to be local Dirichlet problems for the equation (5) with vanishing source term f and boundary values provided by the multiplier.
2. Using the result of the previous step this one reduces to the calculation of

$$\sum_{i=1}^{N} \int_{\partial T_i} m \, \langle \mathbf{j}_i, \boldsymbol{\nu} \rangle \, d\Gamma \qquad \text{for} \quad m \in \mathcal{M} \quad .$$

In order to condense the remaining steps into a single formula we resort to *Poincaré–Steklov operators*, defined to be the Dirichlet–Neumann operators

$$T^i_{\mathrm{DN}} : H^1(T_i) \mapsto H^{-\frac{1}{2}}(\partial T_i) \quad ; \quad p \mapsto e^{\Psi} \frac{\partial u_i}{\partial \boldsymbol{\nu}}$$

They map Dirichlet data on the boundary of a patch T_i via the local problem (16) to the resulting flux through the edges of T_i. The desired formula now reads:

$$\langle Sp, m \rangle_{\mathcal{M}' \times \mathcal{M}} = \sum_{i=1}^{N} \int_{\partial T_i} T^i_{\mathrm{DN}} p \cdot m \, d\Gamma \quad , \quad p, m \in H^1_{\Gamma_D}(\Omega) =: \mathcal{M}$$

The right hand side q can be treated in a similar fashion.

2.2. Spectral Analysis of a Model Problem. The mixed hybrid problem for the Lagrangian multiplier is now more closely examined in the case of a simple model problem which permits an explicit calculation of eigenfunctions. The setting is as follows (see Figure 1):

- Ω is the square $]0,\pi[^2$
- The triangulation $\mathcal{T}$ of Ω consists of two patches $T_1 =]0,\pi[\times]0,h[$ and $T_2 =]0,\pi[\times]h,\pi[$ for $h \in]0,\pi[$ with joint edge $\Gamma_3 := \partial T_1 \cap \partial T_2$
- The analysis is confined to piecewise linear potential, meaning that $\Psi(\mathbf{x}) = \langle \mathbf{c}, \mathbf{x}\rangle \ \forall \mathbf{x} \in \Omega$ with a constant vector $\mathbf{c} := \binom{c_1}{c_2} \in \mathbb{R}^2$.
- We assume $R(\mathbf{x}) = 0$ for all $\mathbf{x} \in \Omega$
- We have homogeneous Dirichlet conditions all over $\partial\Omega$.

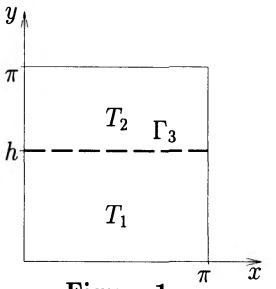

Figure 1

We regard S of (13) as an operator in a space of functions defined on Γ_3 and we are now looking for its eigenfunctions. Since convection–diffusion problems on each subdomain T_1, T_2 are involved at first we have to focus on the operator

$$L : \begin{cases} H^1(D) & \mapsto & H^{-1}(D) \\ n & \mapsto & \Delta n - \langle \mathbf{c}, \nabla n\rangle \end{cases}$$

for an arbitrary domain D. Straightforward calculation shows that for any $\kappa \in \mathbb{R}$ the functions

$$\Psi_\kappa(\mathbf{x}) = e^{\frac{1}{2}\langle \mathbf{c},\mathbf{x}\rangle} \sin(\kappa x) \sinh\left(\sqrt{\kappa^2 + \frac{1}{4}|\mathbf{c}|^2}\, y\right), \quad \mathbf{x} = \begin{pmatrix} x \\ y \end{pmatrix} \in \Omega, \quad \kappa \in \mathbb{R}$$

belong to the kernel of L. Thanks to this result the boundary problems (16) we face as a first step in the evaluation of Sp yield an analytic solution, if the multiplier p on Γ_3 is of the form

$$p_\kappa(x) = e^{\frac{1}{2}c_1 x} \sin(\kappa x), \quad x \in [0,\pi], \quad \kappa \in \mathbb{N}$$

These functions also satisfy the boundary conditions imposed by our current settings. The main difficulty is now overcome; it just takes mere calculation to show that those $p_\kappa(x)$ are eigenfunctions of S. Moreover, we also get the eigenvalues

$$\lambda_\kappa = \sqrt{\kappa^2 + \frac{1}{4}|\mathbf{c}|^2} \left(\frac{\cosh\left(\sqrt{\kappa^2 + \frac{1}{4}|\mathbf{c}|^2}\, h\right)}{\sinh\left(\sqrt{\kappa^2 + \frac{1}{4}|\mathbf{c}|^2}\, h\right)} + \frac{\cosh\left(\sqrt{\kappa^2 + \frac{1}{4}|\mathbf{c}|^2}\, (\pi - h)\right)}{\sinh\left(\sqrt{\kappa^2 + \frac{1}{4}|\mathbf{c}|^2}\, (\pi - h)\right)} \right), \quad \kappa \in \mathbb{N}$$

Oddly enough, this lengthy expression deserves further attention. First the p_κ represent a complete set of eigenfunctions for the one–dimensional convection–diffusion operator

acting on $H^1(\Gamma_3)$, homogeneous boundary conditions provided. Its corresponding eigenvalues are given by $\mu_\kappa := \kappa^2 + \frac{1}{4}|c|^2$: for large κ λ_κ is about twice the square root of μ_κ. Loosely speaking, S behaves like the square root of a 1D convection–diffusion operator. As it was successfully done in the case of purely elliptic problems (see e.g. [4]), these findings can be exploited to construct a preconditioner for the Schur complement system in a domain decomposition framework.

3. Flux–oriented discretization scheme. We now pursue the intriguing idea to find a discretization scheme for problem (1) based on its mixed hybrid formulation (13). In principle we stick to the customary finite element approach of replacing the function spaces by finite dimensional analogues. We have to supply both a finite dimensional space $\mathcal{M}_h$ of ansatz functions and a space $\tilde{\mathcal{M}}_h$ of test functions. They may but do not need to coincide as we do not want to rule out Petrov–Galerkin techniques. In the usual manner approximating finite element spaces $\mathcal{M}_h, \tilde{\mathcal{M}}_h$ are built upon a triangulation $\mathcal{T}$ of Ω. So far any kind of polygonal patches was admitted but from now on we restrict their shapes to triangles and are calling them elements. All other requirements upon $\mathcal{T}$ remain in effect.

We continue with the local definition of approximating finite element functions, developing a representation for a single element. The rash approach to fix the ansatz for the discrete multiplier $p_h \in \mathcal{M}_h$ in the first place is certainly doomed in practice: it is all but impossible to obtain solutions of the local problems (16) that bulked large in the definition of the mixed hybrid problem. A promising remedy lies in role reversal: we recommend to determine a simple solution of (16) first and then to take its values on ∂T_i to build $\mathcal{M}_h$.

We now assume that R vanishes in all of Ω and that the potential Ψ varies only linearly over each element, i.e. $\Psi(\mathbf{x}) = \langle \mathbf{c}_i, \mathbf{x} \rangle$, $\mathbf{x} \in T_i$ with constant $\mathbf{c}_i \in \mathbb{R}^2$. Then, provided that $\mathbf{c}_i \neq 0$, it makes sense to choose

$$\psi_{i,h}(\mathbf{x}) = \alpha \left(\frac{e^{\langle \mathbf{c}_i, \mathbf{x} \rangle} - 1}{|\mathbf{c}_i|} \right) + \beta \langle \mathbf{r}_i, \mathbf{x} \rangle + \gamma, \quad \mathbf{x} \in T_i \tag{17}$$

(in the trivial case $\mathbf{c}_i = 0$, $\psi_{i,h}$ is taken to be an ordinary linear function), with $\mathbf{r}_i$ being any nonzero vector perpendicular to $\mathbf{c}_i$, as a local ansatz for a function in $\mathcal{M}_h$. The very same approximation of the local flux has already been used by Baliga and Patankar in a finite volume scheme (cf. [2]). Our decision in favour of (17) is backed by several observations: Firstly, the discrete flux

$$\mathbf{j}_i(\mathbf{x}) = e^{\Psi} \nabla (e^{-\Psi} \psi_{i,h})(\mathbf{x}) = \beta \mathbf{r}_i - (\beta \langle \mathbf{r}_i, \mathbf{x} \rangle + \gamma - \alpha / |\mathbf{c}_i|)\, \mathbf{c}_i$$

is a "smooth" function and does not change in the direction of $\mathbf{c}_i$. Remember that $\mathbf{c}_i$ is parallel to the electric field to see that $\mathbf{j}_i$ neatly fits the current which does not vary much along electric field lines either. Secondly, the ansatz also meets our original goal of satisfying the local problem what $\operatorname{div} \mathbf{j}_i = 0$ gives evidence for.

Given $\operatorname{div} \mathbf{j}_\iota = 0$, the current ansatz is reminiscent of one proposed by Bank et al. in [3], for it is obviously *divergence-free* and this property carries important consequences: By means of Green's formula we see for $\psi_{\iota,h}$ of type (17) and arbitrary $\phi \in H^1(\Omega)$

$$\begin{aligned}
\langle S\psi_{\iota,h}, \phi\rangle_{\mathcal{M}'(T_\iota)\times\mathcal{M}(T_\iota)} &= \int_{T_\iota} \underbrace{\operatorname{div}(e^{\Psi}\nabla(e^{-\Psi}\psi_{\iota,h}))}_{=0}\, d\mathbf{x} + \int_{T_\iota} \left\langle e^{\Psi}\nabla(e^{-\Psi}\psi_{\iota,h}), \nabla\phi\right\rangle d\mathbf{x} \\
&= \int_{T_\iota} e^{\Psi} \left\langle \nabla(e^{-\Psi}\psi_{\iota,h}), \nabla\phi\right\rangle d\mathbf{x} \\
&= a_{std}(\psi_{\iota,h}, \phi)_{|T_\iota} \qquad \text{in} \quad T_\iota
\end{aligned}$$

with $a_{std} : H^1(\Omega) \times H^1(\Omega) \mapsto \mathbb{R}$ as defined in (3). A related equation can be established for the right hand side of (13): It relies on $\rho_\iota \in H_0^1(T_\iota)$ satisfying

$$\begin{aligned}
\operatorname{div}(e^{\Psi}\nabla(e^{-\Psi}\rho_\iota)) &= f \qquad \text{in} \quad T_\iota \\
\rho_\iota &= 0 \qquad \text{on} \quad \partial T_\iota \quad .
\end{aligned}$$

Due to its shape we dub ρ_ι "bubble". Again an application of Green's formula shows:

$$q(\psi_{\iota,h})_{|T_\iota} = f_{std}(\psi_{\iota,h})_{|T_\iota} - a_{std}(\rho_\iota, \psi_{\iota,h})_{|T_\iota} \qquad \text{in} \quad T_\iota \quad .$$

If we set $\mathcal{M}_h$ to be the space spanned by the functions (17) over all elements, a preliminary result is that the solutions p_h and n_h of the variational problems

$$\begin{aligned}
&\text{Find } p_h \in \mathcal{M}_h \text{ such that } \langle Sp_h, m_h\rangle_{\mathcal{M}'\times\mathcal{M}} = q(m_h)\ , \quad m_h \in \mathcal{M}_h \\
&\text{Find } n_h \in \mathcal{M}_h \text{ such that } a_{std}(n_h + \rho, v_h) = f_{std}(v_h)\ , \quad v_h \in \mathcal{M}_h
\end{aligned}$$

have common values on the edges.

Up to now we have ignored that $\mathcal{M}_h \subset \mathcal{M}$ is violated: Through opting for a simple flux we have sacrificed continuity at interelement boundaries, for tightly welding the $\psi_{\iota,h}$ together would cost us almost all degrees of freedom. Thus we inevitably have to put up with a *nonconforming* method in a narrow sense. Apart from pure continuity there is also a less phenomenological criterion to categorize methods. A discretization is regarded as by nature conforming if source terms are taken into account by jumps of the normal component of the flux across interelement boundaries. Conversely, nonconforming methods usually trade continuity of the solution for n for being more or less flux-conserving. For a reasonably manageable scheme it seems impossible to accommodate both features. In this perspective our divergence-free ansatz can be assigned to the conforming class. Since the flux is the crucial unknown of the continuity equation, we are eager to add some nonconforming flavour. Incorporating the nonconforming principle can be accomplished by enlarging the space. The above calculations provide a clue: They suggest that we add the bubbles ρ_ι as an additional local basis function. In other words, we try $\mathcal{MB}_h := \mathcal{M}_h + \mathcal{B}_h$ with $\mathcal{B}_h := \{\beta_h : \Omega \mapsto \mathbb{R}\,;\ \beta_{h|T_\iota} \in \operatorname{Span}\{\rho_\iota\}\ , T_\iota \in \mathcal{T}_h\}$ as new ansatz space. But the particular appeal of this choice emerges no sooner than one discovers the

relation $a_{std}(m_h, \rho_i) = 0$, $m_h \in \mathcal{M}_h$ meaning that the arising stiffness matrix possesses upper triangular structure if the basis functions are properly arranged. This paves the way for processing source terms independently on each element in advance to calculating the solution on the edges.

We must not gloss over the glaring flaw of the approach described so far: the ρ_i remain elusive. As we are dealing with approximate solutions anyway, we hope to find a simple replacement sufficiently close to ρ_i. For example, the classical cubic bubble scaled by the exponential $e^{1/2\langle \mathbf{c}_i, \mathbf{x}\rangle}$ might be suitable. Also the test space still needs to be specified; pondering experiences obtained for other discretizations we guess that linear test functions can be recommended leading to a Petrov–Galerkin method. All this badly needs empirical underpinning and the results of numerical experiments will be reported in a forthcoming paper.

4. Standard Mixed Finite Element Discretization. Again for simplicity we assume Ω to be a bounded polygonal domain and seek to discretize (11) immediately by means of finite elements. Then with respect to a simplicial triangulation $\mathcal{T} := \{T_i\}_i$ of Ω an appropriate local approximation of the flux space $\mathbf{H}(\mathrm{div}, \Omega, \Gamma_N)$ can be obtained by means of the lowest order Raviart–Thomas element given by

$$\mathcal{RT}_h(T_i) := \{\mathbf{x} \mapsto \mathbf{a} + \beta\mathbf{x}\,;\ \mathbf{x} \in T_i\,,\ \mathbf{a} \in \mathbb{R}^2\,,\ \beta \in \mathbb{R}\}$$

Then we set $\boldsymbol{\mathcal{X}}_h := \bigotimes_i \mathcal{RT}_h(T_i)$ to be the "chopped up" global approximation space for the flux. For each $\mathbf{v}_h \in \mathcal{RT}_h(T_i)$ the divergence $\mathrm{div}\,\mathbf{v}_h$ is constant in T_i and so are its normal traces $\langle \mathbf{v}_h, \boldsymbol{\nu}\rangle_{|e_{i,k}}$ along the edges $e_{i,k}$, $k = 1, 2, 3$ of T_i. For the meaning of the symbols we refer to the figure beside.

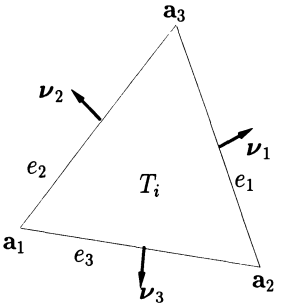

According to famous theoretical results on saddle point problems (Babuška–Brezzi condition, see [5]), we have to choose a locally constant ansatz for $\mathcal{W}_h$. One can easily check that $\mathbf{v}_h \in \mathcal{RT}_h(T_i)$ is uniquely determined by its normal traces on ∂T_i. This hints that the discrete multipliers need only be constant along edges. It takes little more than counting dimensions of the spaces involved to verify that such an $\mathcal{M}_h$ complies with (9). So we have made sure existence and uniqueness of a solution of

Find $(\mathbf{j}_h, n_h, p_h) \in \boldsymbol{\mathcal{X}}_h \times \mathcal{W}_h \times \mathcal{M}_h$ such that

$$\begin{array}{rcrcrcll} a(\mathbf{j}_h, \mathbf{v}_h) & + & b_1(\mathbf{v}_h, n_h) & + & l(\mathbf{v}_h, p_h) & = & g(\mathbf{v}_h)\,, & \mathbf{v}_h \in \boldsymbol{\mathcal{X}}_h \\ b_2(\mathbf{j}_h, w_h) & - & d(n_h, w_h) & & & = & f(w_h)\,, & w_h \in \mathcal{W}_h \\ l(\mathbf{j}_h, m_h) & & & & & = & 0\,, & m_h \in \mathcal{M}_h \end{array} \tag{18}$$

If we partition a comprehensive basis of all approximating spaces according to $(\boldsymbol{\mathcal{X}}_h \times \mathcal{W}_h) \times \mathcal{M}_h$ the associated linear system takes the form

$$\underbrace{\begin{pmatrix} \mathrm{A} & \mathrm{L}_1^T \\ \mathrm{L}_2 & 0 \end{pmatrix}}_{\text{stiffness matrix}} \begin{pmatrix} \vec{z}_h \\ \vec{p}_h \end{pmatrix} = \underbrace{\begin{pmatrix} \vec{r} \\ 0 \end{pmatrix}}_{\text{load vector}} \tag{19}$$

$\vec{z}_h, \vec{p}_h$ are the vectors of unknowns belonging to basis functions in $\boldsymbol{\mathcal{X}}_h \times \mathcal{W}_h$ and $\mathcal{M}_h$, respectively. Please note that now *Lemat* $\neq$ *Lzmat* since the problem in the original unknown n is not symmetric.

4.1. Discrete Hybridization: Implementational Point of View. As pointed out at length the natural treatment of (19) is *static condensation.* What remains is the smaller linear problem

$$\mathrm{S}\vec{p}_h = \mathrm{L}_2\mathrm{A}^{-1}\vec{f} =: \vec{t} \quad \text{with} \quad \mathrm{S} := \mathrm{L}_2\,\mathrm{A}^{-1}\,\mathrm{L}_1^T \tag{20}$$

Thanks to decoupling through the multiplier, A is blockdiagonal and hence cheaply invertible. With the unknowns in $\vec{z}_h$ being eliminated the choice of a particular basis for $\boldsymbol{\mathcal{X}}_h$ and $\mathcal{W}_h$ does not affect S. A basis of $\mathcal{M}_h$ is constructed in a canonical way: Each of its members has support equal to a single edge in $\mathcal{E}_0$.

We do not need to deal with S as a whole: As the Lagrangian multiplier is the only unknown tying together adjoining elements with respect to (19), static condensation can be carried out on the elements' level, provided the bases of $\mathcal{W}_h$ and $\boldsymbol{\mathcal{X}}_h$ are purely local. Our task is thus reduced to calculating 7×7–stiffness matrices and, on these, doing a block elimination of the unknowns belonging to $\mathbf{j}_h, n_h$. After this cumbersome procedure has been finished we have the 3×3–element stiffness matrix for the multipliers, in symbolic notation given by

$$\mathrm{S}_{loc} = -\epsilon^{-1} \begin{pmatrix} |e_1| & & \\ & |e_2| & \\ & & |e_3| \end{pmatrix} \mathrm{U} \begin{pmatrix} \theta_1 & & \\ & \theta_2 & \\ & & \theta_3 \end{pmatrix}$$

where we used the abbreviations

$$\mathrm{U} := (\langle \boldsymbol{\nu}_l, \boldsymbol{\nu}_j \rangle)_{1\le l,j\le 3} \quad , \quad \epsilon := \int_{T_i} e^{-\Psi}\, d\mathbf{x} \quad , \quad \theta_j := \int_{e_j} e^{-\Psi}\, d\Gamma$$

We remark that the formulas above are only valid in the case $R = 0$. For ease of presentation we also forgo the separate treatment of elements attached to the Dirichlet boundary Γ_D.

The element load vector can be expressed by

$$\vec{t}_{loc} = -\frac{1}{2|T_i|} \int_{T_i} f\, d\mathbf{x} \begin{pmatrix} |e_1| & & \\ & |e_2| & \\ & & |e_3| \end{pmatrix} \vec{\zeta}$$

where $\zeta \in \mathbb{R}^3$ and $\zeta_j := \langle \mathbf{p}, \boldsymbol{\nu}_j \rangle - \epsilon^{-1} \int_{T_i} e^{-\Psi} \langle \mathbf{x}, \boldsymbol{\nu}_j \rangle \, d\mathbf{x}$ with $\mathbf{p} \in e_j$. A brief calculation shows that S_{loc} and $\vec{t}_{loc}$ can be read as the stiffness matrix and the load vector of the following local variational problem:

Find $p_h \in \mathcal{M}_h(T_i)$ such that

$$\epsilon^{-1} \left\langle \int_{\partial T_i} m_h \boldsymbol{\nu} \, d\Gamma, \int_{\partial T_i} e^{-\Psi} p_h \boldsymbol{\nu} \, d\Gamma \right\rangle = -\frac{1}{2|T_i|} \int_{\Omega} f \, d\mathbf{x} \cdot \pi(m_h) \, , \quad m_h \in \mathcal{M}_h(T_i) \quad (21)$$

where

$$\pi(m_h) = \int_{\partial T_i} m_h \left\langle \mathbf{x} - \epsilon^{-1} \int_{T_i} e^{-\Psi(\mathbf{x}')} \mathbf{x}' \, d\mathbf{x}', \boldsymbol{\nu} \right\rangle d\Gamma \quad .$$

In practice the rationale behind solving (1) often is to determine the current $\mathbf{j}$ passing through a certain section of the boundary, for example Ohmic contacts. Unfortunately, we just discarded $\mathbf{j}_h$ in the process of static condensation. Therefore, we face the task of retrieving $\mathbf{j}_h$ from the values of the multiplier p_h. First we observe that this again can be done for each element T_i separately. Tedious tinkering with the full 7×7 local stiffness matrix is rewarded by a surprising result: The total flux through the edge of an element is readily available as a component of the residual of the equation $\mathrm{S}_{loc} \vec{p}_{h,loc} = \vec{t}_{loc}$. In this context $\vec{p}_h$ covers three components of $\vec{p}$ which are linked to the edges of T_i. Thus we can obtain the desired fluxes at virtually no extra cost. This should be taken as an additional incentive to search for error estimators based on the flux. It seems wise to do so anyway, considering the pivotal role of the flux in mixed discretization schemes.

4.2. An Equivalent Nonconforming Petrov–Galerkin Ansatz. In section 3, setting out at the mixed hybrid problem, we unexpectedly arrived at a scheme that looked like a modified standard formulation (2). As well the genuine mixed discretization given before can be recast to resemble a variant of (2), though a good deal of twisting is needed. Our presentation partly follows that of Reusken in [12] Again we pick a single element T_i with edges $\{e_1, e_2, e_3\}$, outward normal unit vectors $\{\boldsymbol{\nu}_1, \boldsymbol{\nu}_2, \boldsymbol{\nu}_3\}$ and midpoints $\{\mathbf{m}_1, \mathbf{m}_2, \mathbf{m}_3\}$ of the edges. Furthermore, $R = 0$ is assumed.

Let $\{\phi^1_{i,h}, \phi^2_{i,h}, \phi^3_{i,h}\}$ be the local canonical basis of the Crouzeix–Raviart space $\mathcal{CR}_h$ of linear nonconforming functions given by

$$\phi^k_{i,h}(\mathbf{x}) = \frac{|e_k|}{|T_i|} \langle \mathbf{x} - \mathbf{m}_l, \boldsymbol{\nu}_k \rangle \, , \quad 1 \le k \ne l \le 3 \quad \mathbf{x} \in T_i$$

We additionally require continuity at the midpoints of interelement boundaries and in this case these functions (for all the T_i combined) span the space of test functions. Following the Petrov–Galerkin principle we use the scaled functions

$$\tilde{\phi}^k_{i,h} := \left(\frac{1}{|e_k|} \int_{e_k} e^{-\Psi} \, d\Gamma \right) \phi^k_{i,h} \, , \quad 1 \le k \le 3 \qquad (22)$$

as a local basis of the ansatz space $\tilde{\mathcal{CR}}_h$, from which a global basis is constructed as before.

LEMMA 4.1. *Let $\{\mu^1_{i,h}, \mu^2_{i,h}, \mu^3_{i,h}\}$ be the set of local basis functions of $\mathcal{M}_h$ belonging to the edges of the element T_i. Then*

$$\int_{T_i} \left(\frac{1}{|T_i|} \int_{T_i} e^{\Psi(\mathbf{x}')}\, d\mathbf{x}' \right)^{-1} \left\langle \nabla \tilde{\phi}^k_{i,h}, \nabla \phi^l_{i,h} \right\rangle d\mathbf{x} = \left(\int_{T_i} e^{-\Psi}\, d\mathbf{x} \right)^{-1} \left\langle \int_{\partial T_i} \mu^l_{i,h} \boldsymbol{\nu}\, d\Gamma, \int_{\partial T_i} e^{-\Psi} \mu^k_{i,h} \boldsymbol{\nu}\, d\Gamma \right\rangle$$

holds for $1 \le k, l \le 3$. The functional $\pi : \mathcal{M}_h(T_i) \mapsto \mathbb{R}$, defined in (21), satisfies

$$\pi(\mu^k_{i,h}) = -\int_{T_i} \left(e^{-\Psi(\mathbf{x})} \left(\frac{1}{|T_i|} \int_{T_i} e^{-\Psi(\mathbf{x}')}\, d\mathbf{x}' \right)^{-1} - 3 \right) \phi^k_{i,h}\, d\mathbf{x}\,, \quad 1 \le k \le 3$$

These relations give ample hint about how to alter a_{std} and f_{std} of (2) in such a way that the new forms can describe the variational problem (21):

$$\begin{aligned} a_{mod}(u,v) &= \sum_i \int_{T_i} \left(\tfrac{1}{|T_i|} \int_{T_i} e^{-\Psi}\, d\mathbf{x}' \right)^{-1} \langle \nabla u, \nabla v \rangle\, d\mathbf{x} \\ f_{mod}(v) &= \sum_i \tfrac{1}{2|T_i|} \int_{T_i} f\, d\mathbf{x} \cdot \int_{T_i} \left(e^{-\Psi} \left(\tfrac{1}{|T_i|} \int_{T_i} e^{-\Psi}\, d\mathbf{x}' \right)^{-1} - 3 \right) v\, d\mathbf{x} \end{aligned} \tag{23}$$

With these tailored expressions we finally have:

THEOREM 4.2. *The stiffness matrix arising from the discrete variational problem*

$$\textit{Find } u_h \in \tilde{\mathcal{CR}}_{h\,|\Gamma_D} \textit{ such that } \quad a_{mod}(u_h, v_h) = f_{mod}(v_h)\,, \quad v_h \in \mathcal{CR}_{h\,|\Gamma_D}$$

is equal to the stiffness matrix S *of (20) if we build the test space from the canonical nodal basis of the lowest order Crouzeix–Raviart space and the ansatz space from their scaled counterparts (22).*

The conspicuous term

$$\left(\frac{1}{|T_i|} \int_{T_i} e^{-\Psi}\, d\mathbf{x} \right)^{-1}$$

in (23) is the definition of the harmonic average of the function e^{Ψ} over T_i. To this expression an important class of discretization schemes for the continuity equations (1), namely the *inverse averaging type methods*, owes its name. We consider it satisfactory that mixed methods belong to this prominent club that also includes the widely used Scharfetter–Gummel scheme.

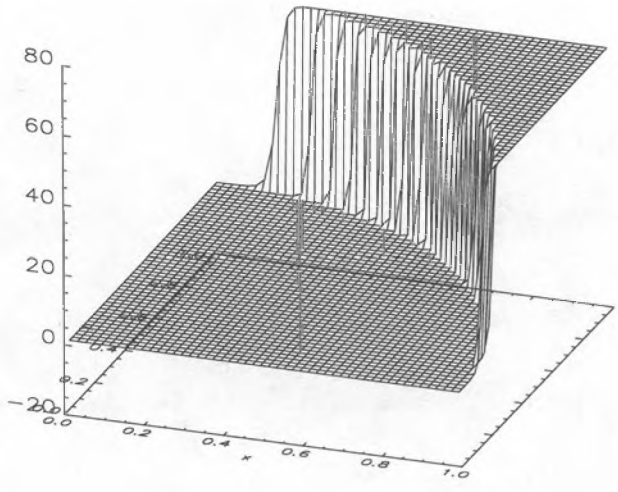

Figure 2: Exact solution for first experiment

5. Numerical experiments. Though general convergence estimates for standard mixed discretizations are available (cf. [1], [6]) they give little insight into the actual performance of the methods in practice. Too many details of their behaviour and qualitative phenomena still defy a theoretical explanation, let alone prediction. So we have to rely on numerical experiments to probe the quality of the method when applied to the continuity equation (1). In semiconductor device simulation the particular challenge of (1) is posed by the layer behaviour of the potential Ψ: Steep gradients occur near pn–junctions whereas Ψ is only slightly varying elsewhere. In order to model these conditions we used the "radial step potential" $\Psi(\mathbf{x}) = \sigma_a(r), r = \sqrt{x_1^2 + x_2^2}, \mathbf{x} = (x_1, x_2) \in \Omega, \sigma_a(r) = 1/(1 + e^{-a(r-1)})$. The parameter a governs the slope of the step: the larger a the sharper the drop. All calculations were carried out on $\Omega =]0, 1[^2$. If necessary, linear interpolation of Ψ and f was used and all linear systems have been solved exactly.

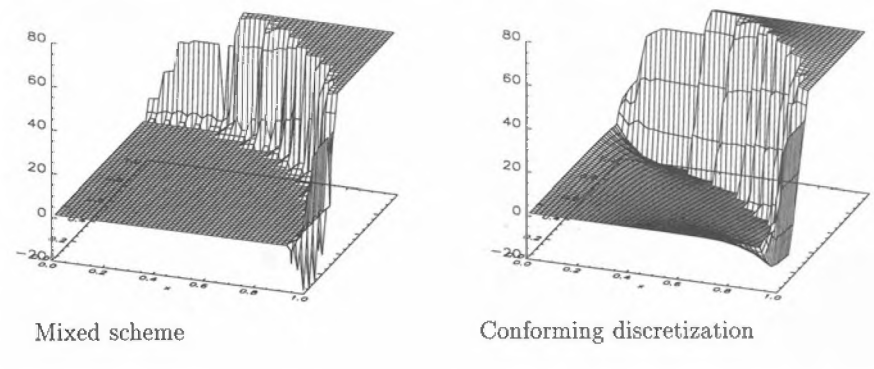

Figure 3: Approximate solutions for first experiment

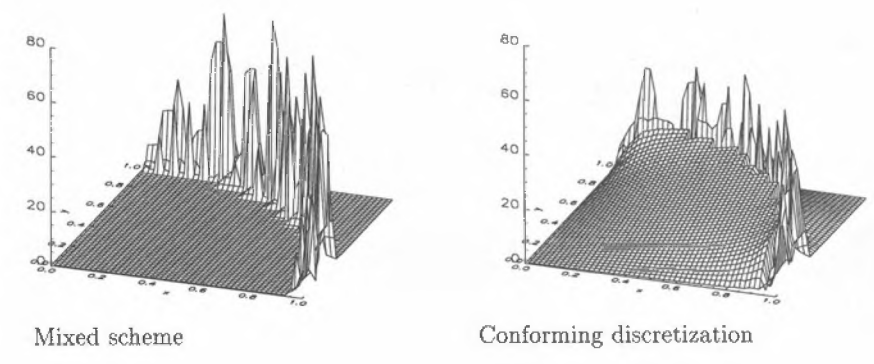

Figure 4: Absolute errors of approximate solutions of first experiment

For a first experiment Ω was triangulated by a rectangular grid of mesh width $h = \frac{1}{16}$ with each cell being further subdivided into two triangles. The radial step potential with $a = 500$ and vanishing right hand side were employed, along with boundary values that yield e^{Ψ} as exact solution. In physical parlance this situation is referred to as thermal equilibrium. We solved the problem by our mixed method and compared the solution and the errors with those obtained by using standard conforming linear elements. The figures 2 through 5 give a graphical representation of the results.

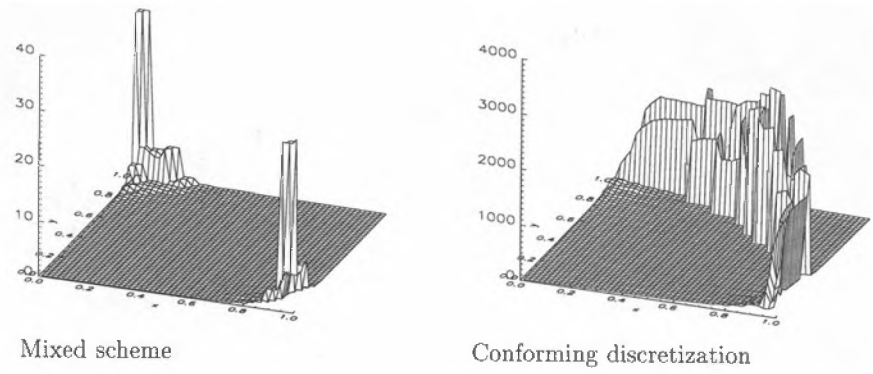

Figure 5: Absolute errors of the flux for first experiment

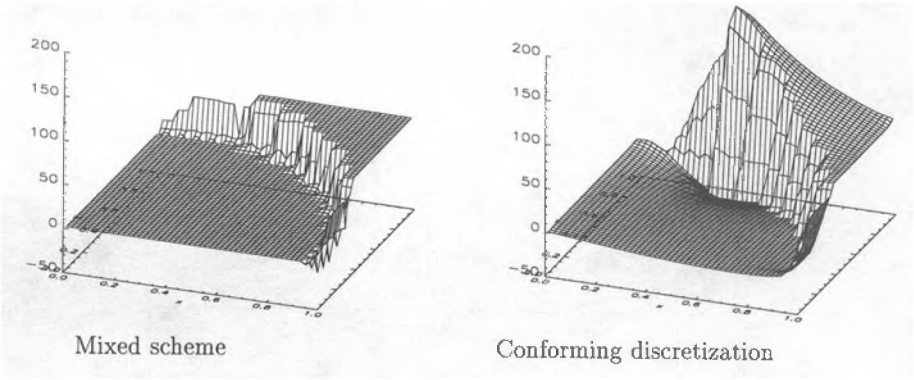

Figure 6: Approximate solution for 2nd experiment. (Two Neumann sides)

We see that the mixed discretization benefits from the very smooth, actually vanishing flux in this experiment. It copes with the internal layer of the solution for n far better than the conforming method and flatly outstrips the latter with respect to reproducing the zero flux. It should be noted that presumably not the method itself but post-processing has to be blamed for the spurious spikes that pop up close to the step. Perhaps this taint can be removed by a more refined post-processing that includes bubble functions as investigated in [1]. The mixed method may perform strikingly better in this setting, but that does the method only small credit, because the comparison is not quite fair, as the conforming discretization are prone to failure in the presence of dominating convection.

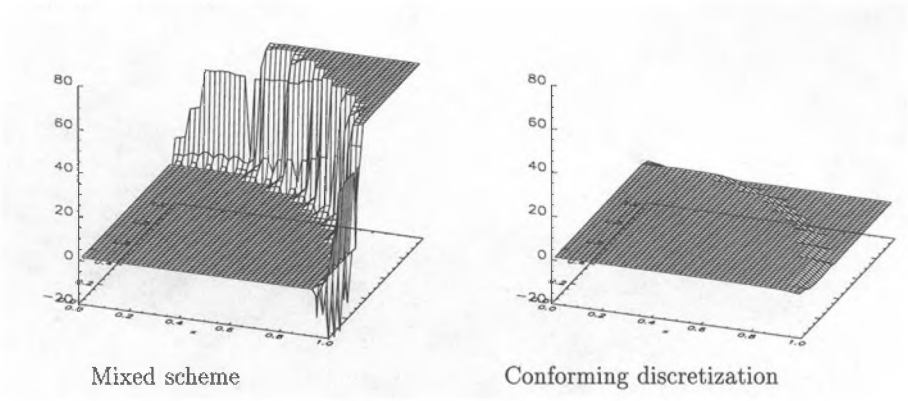

Figure 7: Approximate solution for 2nd experiment. (Three Neumann sides)

The next experiment was designed to investigate the impact of boundary conditions. The setting remained unchanged except that Neumann boundary conditions were imposed on one or more sides of Ω. The figures 6 and 7 show how both methods respond to additional Neumann boundary parts.

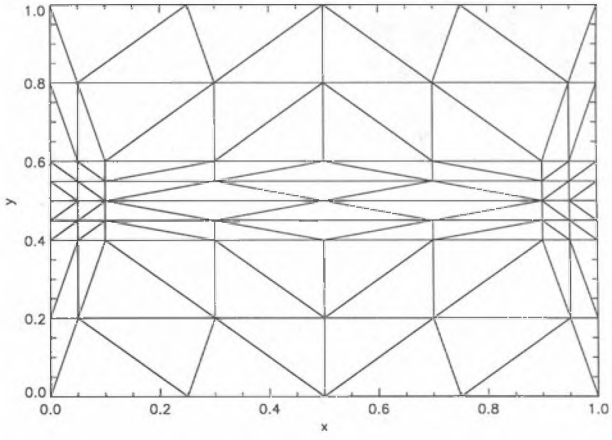

Figure 8: Triangulation with obtuse elements

The mixed solution turns out to be scarcely affected by changing boundary conditions. Conversely, the conforming approximation quickly deteriorates when the size of the Neumann boundary portions increases. This is hardly surprising, because at Neumann boundaries the flux is fixed and so is one unknown of the mixed ansatz. This accounts for the

stabilizing effect of large Neumann parts on the mixed approximation.

Flux oriented discretizations are notorious for their vulnerability to "badly" shaped elements that have an obtuse angle. To expose this shortcoming of the mixed method we built a triangulation with obtuse elements in one part of the domain (See Figure 8), which was then regularly refined twice. This (third) experiment was conducted with a linear potential $\Psi(\mathbf{x}) = \langle \mathbf{c}, \mathbf{x} \rangle, \mathbf{c} \in \mathbb{R}^2$. The boundary values and right–hand side were adjusted to yield a polynomial solution. The distribution of different kinds of errors for three different directions $\mathbf{c}$ of the convection is displayed in figures 9, 10 and 11. Figure 12 shows how the presence of wretched elements leads to distortions in the calculated flux for a particular choice of $\mathbf{c}$. Besides we measured how errors depend on the direction of $\mathbf{c}$. $\mathbf{c}$ had length 100 and in very small steps was fully rotated around the origin (α denotes the angle relative to the abscissa.). The result is plotted in figure 13.

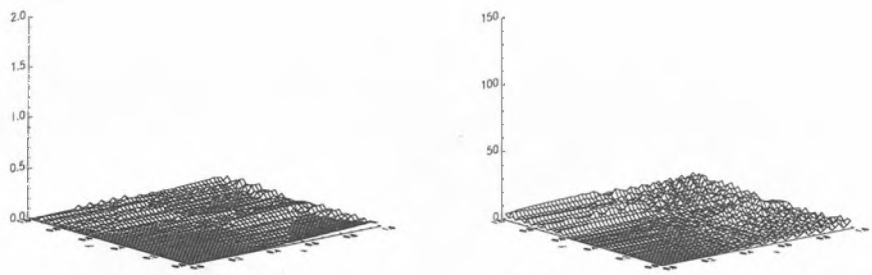

Absolute local error

Absolute local error of the flux

Figure 9: Results of experiment 3 with $\mathbf{c} = \binom{100}{0}$

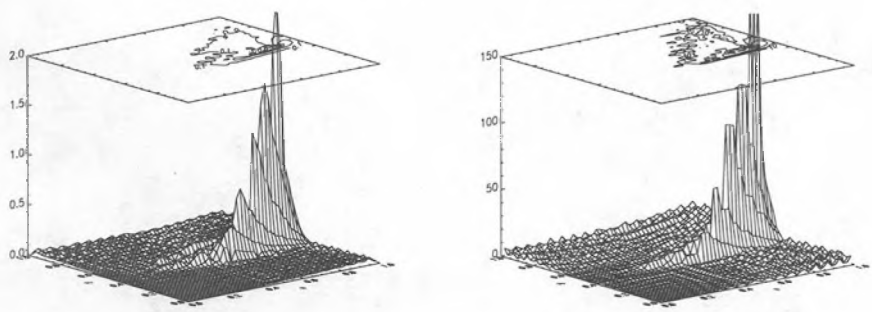

Absolute local error

Absolute local error of the flux

Figure 10: Results of experiment 3 with $\mathbf{c} = \binom{70}{70}$

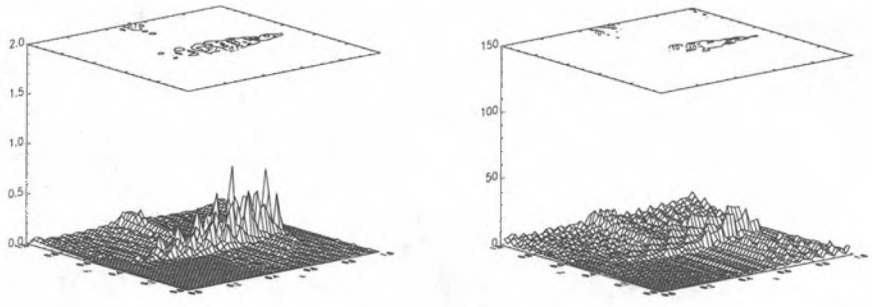

Absolute local error

Absolute local error of the flux

Figure 11: Results of experiment 3 with $\mathbf{c} = \binom{0}{100}$

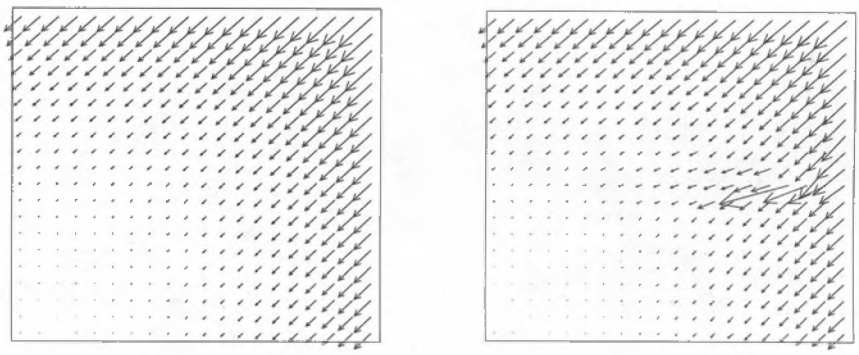

Exact flux

Calculated flux

Figure 12: Exact and calculated flux for $\mathbf{c} = \binom{70}{70}$

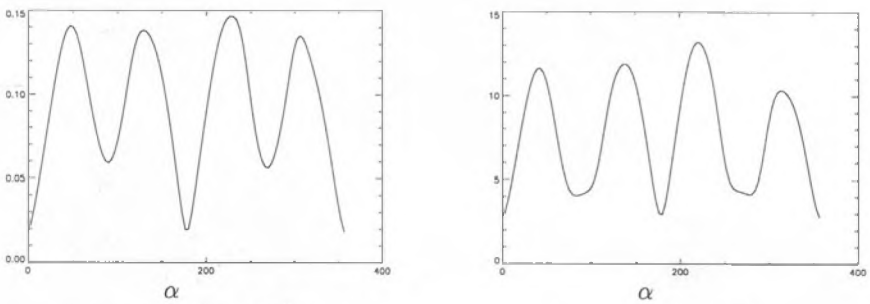

Error norm $\|n - n_h\|_{L^2}$

Error norm $\|\mathbf{j} - \mathbf{j}_h\|_{\mathbf{L}^2}$

Figure 13: L^2–Norm of the error depending on α for experiment 3

The results teach that for some values of **c** obtuse angles might cause disastrous instability. The plots also reveal that in these cases large errors spread to parts of the domain where the triangulation is not "marred", that is, a sort of pollution effect is present. Apparently other directions of **c** do no harm; we see an enigmatic relationship between error and direction of convection: Maybe a clever orientation of the obtuse elements can help to steer clear of the instability trap. Nevertheless, the results send a daunting message as far as an adaptive strategy is concerned: While for plane problems clever refinement strategies for triangulations exist that avoid obtuse elements, in 3–D simulation they inevitably occur. The viability of the mixed method in practice hinges on whether instability can be managed.

REFERENCES

[1] D. N. ARNOLD, F BREZZI, *Mixed and Nonconforming Finite Element Methods: Implementation, Post-Processing and Error Estimates*, Math Modelling Numer Anal , **19**, 7–35 (1985)

[2] B. R. BALIGA, S V. PATANKAR, *A New Finite Element Formulation for Convection-Diffusion Problems*, Numerical Heat Transfer, **3**, 393–409 (1980)

[3] R.. BANK, J. BÜRGLER, W. FICHTNER, R. K SMITH, *Some Upwinding Techniques for Finite Element Approximations of Convection-Diffusion Equations*, Num. Math, **58**, 185–202 (1990)

[4] P.. BJØRSTAD, O. B. WIDLUND, *Iterative Methods for the Solution of Elliptic Problems on Regions Partitioned into Substructures*, SIAM J. Numer Anal., **23**, 1097–1120

[5] F. BREZZI, *On the Existence, Uniqueness and Approximation of Saddle Point Problems Arising from Lagrangian Multipliers*, R A I R.O Anal. Numer , **8**, 129–151

[6] F. BREZZI, M. FORTIN, *Mixed and Hybrid Finite Element Methods*, Springer– Verlag, New York (1991)

[7] F BREZZI, L D MARINI, P PIETRA, *Two Dimensional Exponential Fitting and Application to Drift-Diffusion Models*, SIAM J. Numer. Anal , **26**, 1347–1355 (1989)

[8] ——, *Numerical Simulation of Semiconductor Devices*, Comp Math. Appl Mech Eng , **75**, 493–514 (1989)

[9] I EKELAND, R. TEMAM, *Convex Analysis and Variational Problems*, North–Holland, Amsterdam (1978)

[10] T J R HUGHES, A. BROOKS, *Streamline-Upwind Petrov-Galerkin Formulations for Convective Dominated Flows with particular Emphasis on the Incompressible Navier Stokes Equations*, Comput. Methods Appl Mech. Eng , **32**, 199–259 (1982)

[11] P. A RAVIART, J. M THOMAS, *A Mixed Finite Element Method for Second Order Elliptic Problems*, Lecture Notes in Mathematics, **606**, Springer–Verlag, Berlin (1977)

[12] A REUSKEN, *Multigrid Applied to Mixed Finite Element Schemes for Current Continuity Equations*, Preprint Technical University Einhoven (1990)

[13] VEUBEKE, B. FRAEIJS DE, *Displacement and Equilibrium Models in the Finite Element Method* in "Stress Analysis" (O. C Zienkiewicz, G Hollister, eds), John Wiley and Sons, New York (1965)